Central Memory CD4+ T Cells Are Responsible for the Recombinant Bacillus Calmette-Guérin Δ*ureC*::*hly* Vaccine's Superior Protection Against Tuberculosis

Alexis Vogelzang,[1] Carolina Perdomo,[1] Ulrike Zedler,[1] Stefanie Kuhlmann,[1] Robert Hurwitz,[2] Martin Gengenbacher,[1,a] and Stefan H. E. Kaufmann[1]

[1]Department of Immunology, and [2]Core Facility Protein Purification, Max Planck Institute for Infection Biology, Berlin, Germany

Bacillus Calmette-Guérin (BCG) has been used for vaccination against tuberculosis for nearly a century. Here, we analyze immunity induced by a live tuberculosis vaccine candidate, recombinant BCG Δ*ureC*::*hly* vaccine (rBCG), with proven preclinical and clinical safety and immunogenicity. We pursue in-depth analysis of the endogenous mycobacteria-specific CD4+ T-cell population, comparing the more efficacious rBCG with canonical BCG to determine which T-cell memory responses are prerequisites for superior protection against tuberculosis. rBCG induced higher numbers and proportions of antigen-specific memory CD4+ T cells than BCG, with a CXCR5+CCR7+ phenotype and low expression of the effector transcription factors T-bet and Bcl-6. We found that the superior protection of rBCG, compared with BCG, correlated with higher proportions and numbers of these central memory T cells and of T follicular helper cells associated with specific antibody responses. Adoptive transfer of mycobacteria-specific central memory T cells validated their critical role in protection against pulmonary tuberculosis.

Keywords. BCG; Δ*ureC*::*hly*; VPM1002; vaccine; *Mycobacterium tuberculosis*; memory T cells.

Bacillus Calmette-Guérin (BCG), an attenuated vaccine strain derived from virulent *Mycobacterium bovis*, has been in use as a vaccine against tuberculosis for nearly a century [1]. Vaccination in early childhood induces an immune response to *Mycobacterium tuberculosis*, which prevents disseminated miliary and meningeal forms of the disease. However, protection against the common pulmonary tuberculosis that affects people of all age groups is insufficient [2]. Thus, there is an urgent need for novel vaccines that (1) induce efficacious protection against tuberculosis and (2) are also safe in human immunodeficiency virus (HIV)+ individuals, in whom an otherwise harmless live vaccine can cause disseminated disease [3, 4].

Early animal studies of BCG identified CD4+ T cells as key elements underlying immunological memory against subsequent challenge with *M. tuberculosis* [5, 6]. Adoptively transferred transgenic CD4+ T cells specific for antigen (Ag) 85B (Ag85B; Rv1886c), also expressed by BCG, are capable of controlling a chronic bacterial load in *M. tuberculosis*–infected lungs [7, 8]. CD4+ T cells are a heterogeneous population composed of effector and memory (T_M) subtypes coexpressing a variety of cytokines, chemokines, and receptors with varying impact on protective immunity [9, 10]. The early appearance of T-helper 1 (Th1) type CD4 effector memory T cells (T_{EM}) secreting interferon γ (IFN-γ)/tumor necrosis factor α (TNF-α) has been considered crucial

for orchestration of protective immunity in the infected lung, but recently, it has been questioned whether expression of these pro-inflammatory mediators in the lung is indeed sufficient for control of tuberculosis [11, 12]. Systemic maintenance of T_M following vaccination and their recruitment to the lung following infection remains a key focus of vaccine and biomarker studies [13, 14].

The tuberculosis vaccine candidate containing recombinant BCG ΔureC::hly (rBCG; VPM1002), which secretes pore-forming listeriolysin (hly), has proven its clinical safety and immunogenicity [15, 16]. Here, we pursue an in-depth analysis of the endogenous mycobacteria-specific T_M, comparing the more efficacious rBCG with canonical BCG to determine which T_M responses are prerequisites for superior protection against tuberculosis. It remains challenging to effectively analyze the kinetics and components of the spatially diffuse immune response in humans or animal models induced by BCG, as live bacteria can disseminate to disparate organs in different individuals. We harnessed a sensitive technique in which peptide major histocompatibility complex (MHC) class II tetramer$^+$ T cells were enriched from pooled secondary lymphoid organs of vaccinated mice. This approach allowed us to precisely quantify the kinetics of specific CD4$^+$ T cells following vaccination and subsequent *M. tuberculosis* aerosol challenge and to identify specific central memory T cells (T_{CM}) as mediators against pulmonary tuberculosis.

MATERIALS AND METHODS

M. tuberculosis and BCG Culture
BCG SSI 1331 (American Type Culture Collection [ATCC]; no. 35733), rBCG, and *M. tuberculosis* H37Rv (ATCC; no. 27294) were prepared as described previously [17]. For colony-forming unit (CFU) enumeration, serial dilutions were performed in phosphate-buffered saline containing 0.05% Tween 80 and plated onto Middlebrook 7H11 agar. Plates were incubated at 37°C for 3–4 weeks prior to counting.

Animals and Infections
All experimental procedures involving mice were performed in accordance with requirements of and approval by the State Office for Health and Social Services (Landesamt für Gesundheit und Soziales), Berlin, Germany. C57BL/6 mice were purchased from Charles River Laboratories (Germany), and P25 Tg [7] and B6PL lines from Jackson Laboratories (USA) were bred in house. Mice were 8–12 weeks old, matched for age and sex, and kept under specific pathogen-free conditions. Vaccines (0.5–1.0 × 10^6 CFU BCG or rBCG in 100 ul phosphate buffered saline) were delivered subcutaneously at the tail base. A Glas-Col inhalation exposure system was used for aerosol infection of mice with low-dose (150–200 CFU) *M. tuberculosis*, confirmed by plating lung homogenates 1 day after infection.

Tetramer-Based Cell Enrichment and Flow Cytometry
I-Ab:Ag85B (280–294: FQDAYNAAGGHNAVF) tetramers were provided by the National Institutes of Health (NIH) tetramer facility (USA), I-Ab:ESAT-6 (1–20: MTEQQWNFA-GIEAAASAIQG) tetramers were made in house. A total of 10 nM of Ag85B tetramer was added to single-cell suspensions of pooled spleen and lymph nodes (LNs; cervical, retromaxillary, inguinal, peripheral, and mesenteric) or lung cells for 1 hour at room temperature. For memory phenotyping, 2 µg of CXCR5 (2G8; Becton Dickinson) and CCR7 (5B12 RUO) antibodies (Ab) were included. Tetramer$^+$ cells were enriched according to a published protocol [18]. In brief, samples were incubated with magnetic antifluorochrome microbeads and run through an LS column (Miltenyi Biotec), and the resulting cell fractions were analyzed by flow cytometry. All Ab were from eBioscience, unless otherwise noted. For identification of surface markers, the sample was stained on ice with Ab specific for B220 (RA3-6B2), CD11b (MI-70), CD11c (N418), CD8α (5H10; Invitrogen, Carlsbad, CA), PD-1 (J43), CD4 (RM4-5), CD3ε (145-2C11), CD44 (IM7), CD90.1 (HIS51), and/or CD90.2 (53-2.1). Intracellular staining with Ab for Foxp3 (FJL-16s), RORγt (B2D), T-bet (ebio4B10), and Bcl-6 (7D1, Santa Cruz) was performed with Foxp3 fixation/permeabilization buffers (eBioscience) in accordance with the manufacturer's instructions. Analysis was performed on an LSR II or FACS Canto II (Becton Dickinson) flow cytometer. Data were analyzed with FlowJo (TreeStar).

Isolation of Lung-Resident Lymphocytes
Lungs were harvested from perfused animals and digested with collagenase (0.7 mg/mL Collagenase IV [Sigma-Aldrich] and 0.3 mg/mL Collagenase D [Roche]) in complete Roswell Park Memorial Institute (RPMI) 1640 medium complemented with 10 µg/mL brefeldin A (Santa Cruz) at 37°C in 5% CO$_2$ for 30 minutes. Single-cell suspensions were prepared by mechanical dissociation through a 70-µm nylon mesh in RPMI 1640 medium (with 10% fetal calf serum [Gibco], penicillin/streptomycin, and brefeldin A].

Adoptive Cell Transfer
Spleens and LNs were pooled from 10 rBCG-vaccinated donor mice at day 15, and APC-Ag85B:I-Ab CD4$^+$ T cells were enriched with anti-APC beads over a magnetic column (Miltenyi Biotec) prior to cell sorting using a FACS Aria II. Endogenous or P25 Ag85B-specific T_{EM}, T_{CM}, or T_{FH} at >85% purity were injected intravenously into recipient mice. Naive Tg P25 cells were enriched from the pooled LNs from CD90.1$^+$ congenic mice, using a CD4$^+$ T-cell isolation kit (Miltenyi Biotec).

Enzyme-Linked Immunosorbent Assay (ELISA)
Multisorb ELISA plates (NUNC) were coated overnight with 2 µg/mL of protein lysate prepared by sonicating log-phase

H37Rv *M. tuberculosis*. Nonspecific binding was blocked by preincubation for 2 hours with 3% bovine serum albumin (BSA). Serial dilutions were added to the plate prepared in 1% BSA in phosphate-buffered saline for 2 hours, followed by washing and detection of OD by use of alkaline phosphatase–conjugated isotype-specific secondary Ab (Southern Biotech).

Statistical Analysis

GraphPad Prism software (USA) was used for statistical analysis. Bacterial titers were analyzed by the nonparametric Mann–Whitney test. Frequencies and numbers of specific cells were compared using a 2-way Student *t* test or 1-way analysis of variance, followed by the Bonferroni posttest.

RESULTS

Increased Ag-Specific CD4+ T-Cell Responses Induced by rBCG, Compared With Those Induced by Canonical BCG

rBCG provides superior protection against aerosol challenge with *M. tuberculosis* [16]. Moreover, rBCG has an improved safety profile, showing diminished persistence following subcutaneous vaccination of C57BL/6 mice (Figure 1) [15]. rBCG also disseminated rarely to peripheral lymphoid organs such as the spleen and never disseminated to the lung (Figure 1). BCG induces T_M responses to shared mycobacterial Ag, which can enhance and accelerate the immune response following subsequent challenge with *M. tuberculosis* [19]. To characterize CD4+ T-cell responses to rBCG, an MHC class II tetramer of Ag85B-derived peptide (Ag85B:I-Ab) was used to enrich the CD44^{lo} naive repetoire from untreated controls (mean cell count [±standard error of the mean {SEM}], 87 ± 21 cells), and the expanded population from vaccinated animals (Figure 2A). rBCG drove superior expansion, which persisted 3 months after clearance of the vaccine and contraction of the immune response (mean cell count [±SEM], 662 ± 190.8 cells in BCG recipients and 1625 ± 379.8 cells in rBCG recipients at

day 84; n = 10; Figure 2B). The increased T-cell number was confirmed at the polyclonal level by measuring the proportion of CD4+ T cells that upregulated CD154 in an Ag-specific manner after stimulation with mycobacterial lysate (Supplementary Figure 1) [20]. We conclude that rBCG induced a quantitative increase in CD4+ T cells specific for mycobacterial Ag.

Effector CD4+ T-Cell Migration to the Lung Following Vaccination Echoes Systemic Expansion

The systemic dynamics of Ag-specific CD4+ T-cell responses were recapitulated in the peripheral target organ, the lung, where subcutaneous administration of rBCG at the tail base also induced increased numbers and proportions of Ag85B-specific CD4+ T cells, compared with BCG (Figure 3). Rare Ag-specific T cells could be detected above background without enrichment only at the peak of the response at 14 days after receipt of rBCG (Figure 3), suggesting that neither vaccine generated a pool of mucosa-resident T_{EM}, perhaps surprisingly despite occasional dissemination following BCG but not rBCG vaccination (Figure 1). Thus, the T_M generated by subcutaneously administered BCG or rBCG are maintained over the long term in the secondary lymphoid organs, rather than in the lung.

rBCG Induces Elevated T_{CM} and Follicular Helper T-Cell (T_{FH}) Differentiation of CD4+ T Cells

In addition to the quantitative increase in Ag-specific T cells in rBCG recipients, compared with BCG recipients, enriched Ag85B:I-Ab+ cells expressed different T_M lineage surface markers. While both vaccines generated similar numbers of T_{EM} (CCR7−CXCR5−PD-1−), rBCG increased the number of T_{CM} (CCR7+CXCR5+PD-1+) during the peak of the response (Figure 4A). As viable rBCG is quickly cleared in the first weeks following receipt in C57BL/6 mice, we suspected that persistence of Ag85B-specific T cells was due to the establishment of a pool of T_{EM} and T_{CM}, rather than to T_H maintained by the presence
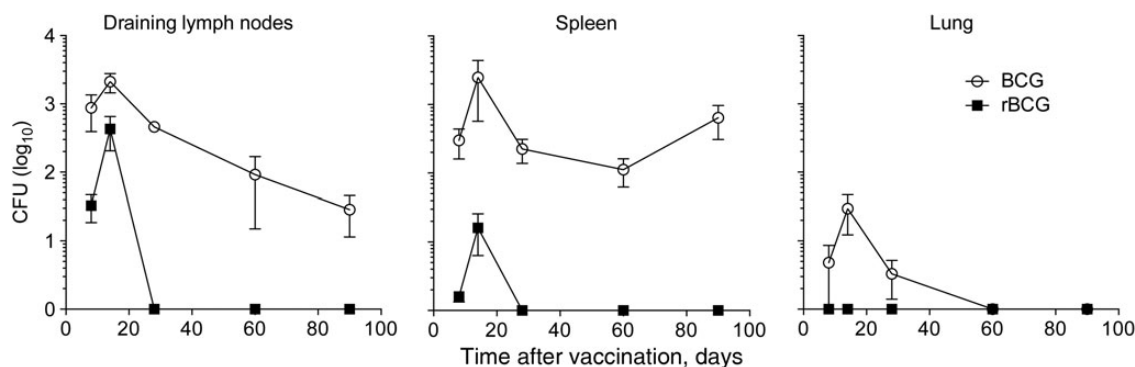

Figure 1. Kinetics of bacillus Calmette Guerin (BCG) and recombinant BCG (rBCG) clearance. Mice were vaccinated with either BCG or rBCG subcutaneously on day 0. Shown are mean colony-forming units (CFU; ± standard error of the mean) of 2 pooled experiments (n = 10).
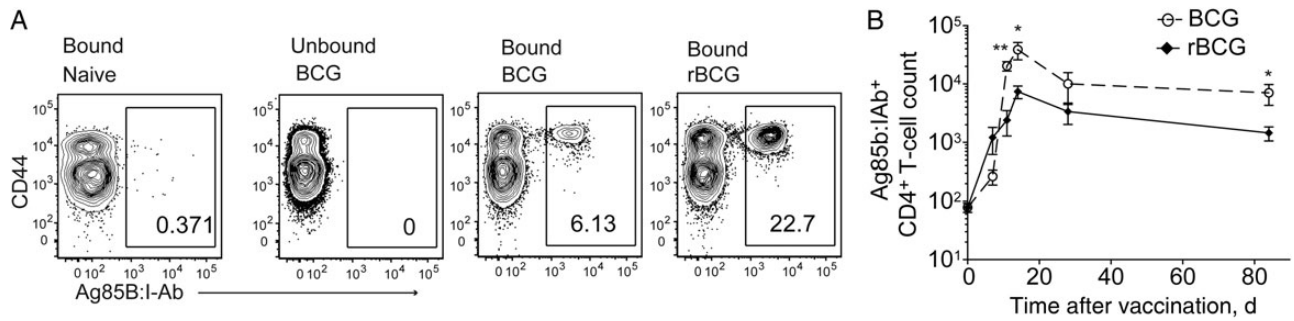
Figure 2. Kinetics of endogenous CD4$^+$ T-cell responses in secondary lymphoid organs following BCG or rBCG vaccination. *A*, Flow cytometry of magnetic column–bound and unbound fractions following enrichment of Ag85B:I-Ab$^+$ CD4$^+$ T cells, gated on CD3$^+$CD4$^+$ T cells, from pooled lymph nodes and spleens obtained from individual naive controls or 14 days after vaccination, as described in Figure 1. *B*, Total numbers of Ag85B:I-Ab$^+$ CD4$^+$ T cells in pooled secondary lymphoid organs. Data are representative values (*A*) or pooled values from 3 independent experiments (*B*; n = 12). *$P < .05$ and **$P < .01$, by a 2-tailed Student *t* test.

of live bacteria, but discriminating between the T$_{EM}$ and T$_{CM}$ phenotypes from effector Th1 and T$_{FH}$ responses is challenging by means of surface phenotype alone. Numerical increase of specific T$_{FH}$ following rBCG vaccination was identified on the basis of their very high expression of the surface markers, CXCR5 and PD-1 (CCR7$^+$CXCR5^{hi}PD-1^{hi}), and the increased intracellular abundance of the germinal center–associated transcription factor Bcl-6 [21], compared with other T$_M$ subsets (Figure 4*B* and 4*C*). However, Ag-specific T cells in rBCG recipients displayed a lower abundance of other indicators of effector phenotype differention, such as Th1 effector transcription factor T-bet that drives IFN-γ/TNF-α secretion (Figure 4*C*) [22].

Furthermore, cytokine secretion was only rarely detected in Ag-specific CD4$^+$ T cells isolated ex vivo from BCG recipients, even at the peak of the response, as has been previously shown for Ag-specific T cells following *M. tuberculosis* infection (data not shown) [23]. Specific CD4$^+$ T-cell expression of T regulatory, T$_{H17}$, or T$_{FH}$ transcription factors FoxP3, RORγt, or Bcl-6 [24], respectively, was negligible following both vaccination regimens, supporting the notion that these cells reflected a memory rather than an effector phenotype (Figure 4*C*). After 3 months, specific CD4$^+$ T cells enriched from secondary lymphoid organs from BCG or rBCG recipients exhibited distinct ratios of memory subsets: rBCG drove greater expansion and persistence of
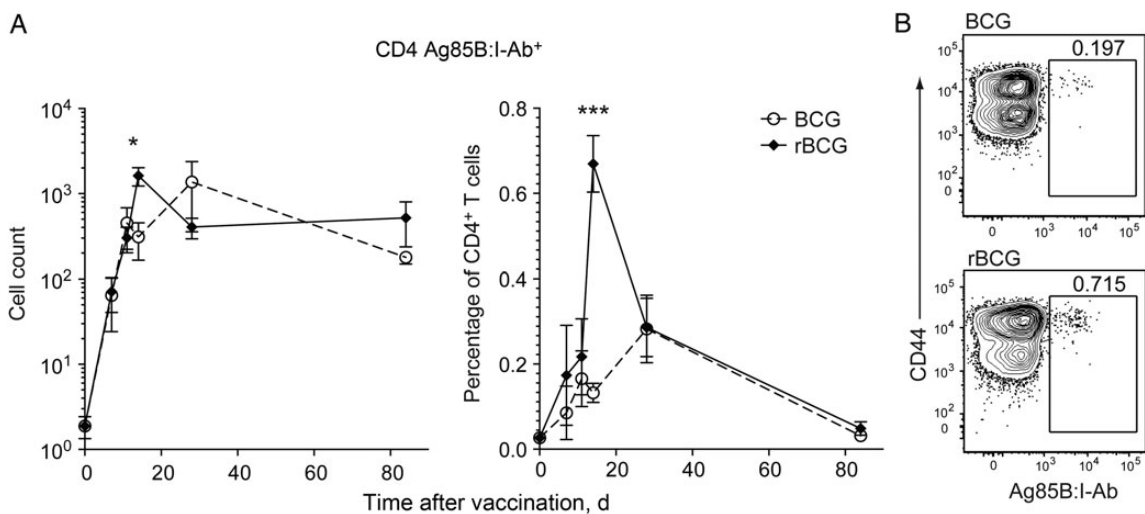

Figure 3. Antigen-specific CD4$^+$ T cells migrate to the lung following subcutaneous BCG or rBCG vaccination. *A*, Numbers and frequencies of unenriched Ag85B:I-Ab$^+$ CD4$^+$ T cells in lung. *B*, Representative flow cytometry of the percentage of Ag85B:I-Ab$^+$ CD4$^+$ T cells in lung, gated on CD3$^+$CD4$^+$ T cells, 14 days after vaccination as described in Figure 1. Data are mean values (± standard error of the mean) of pooled samples (*A*) or representative values from individual mice from 2–3 experiments (*B*; n = 8–12). *$P < .05$ and ***$P < .001$, by a 2-tailed Student *t* test.
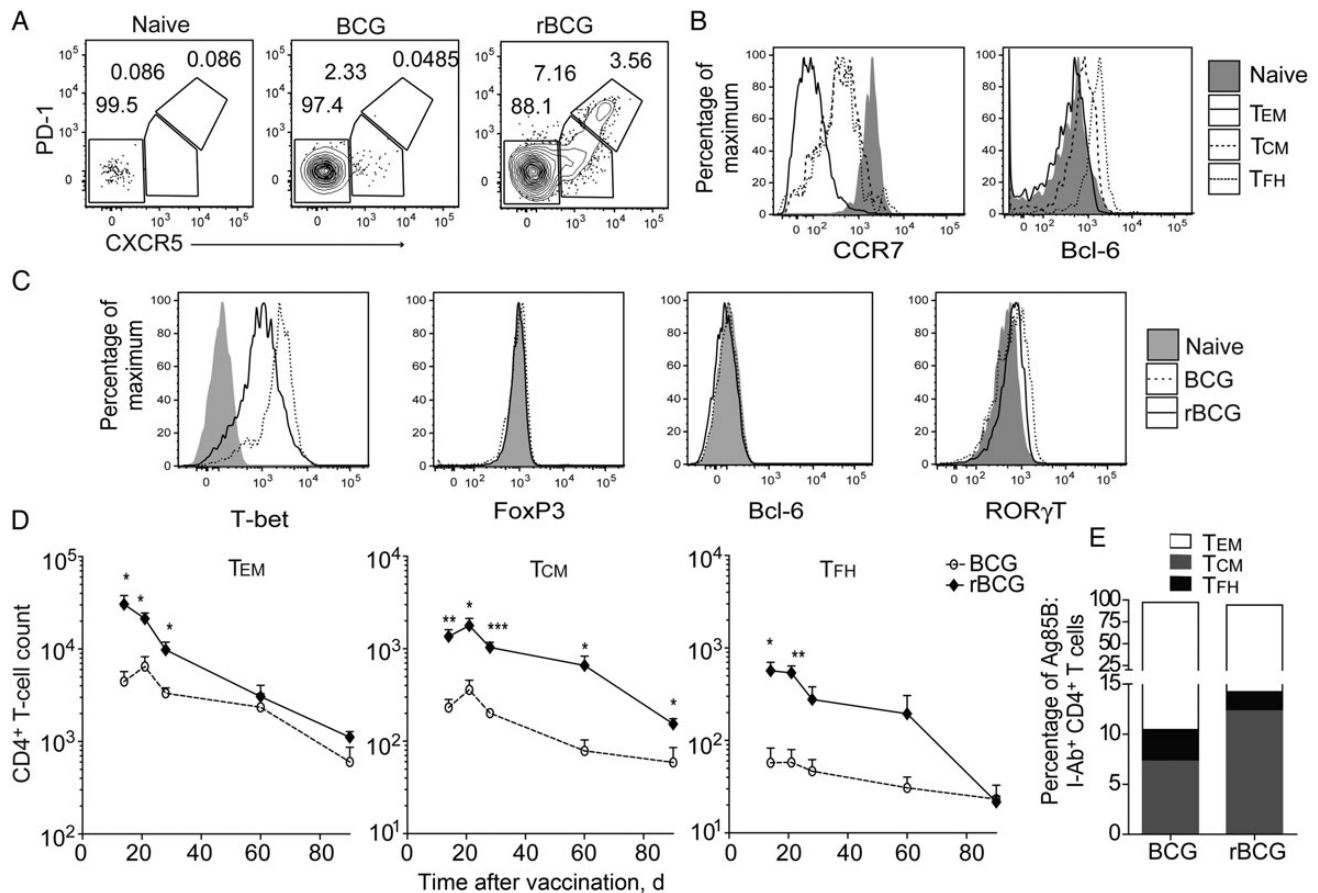
Figure 4. Vaccination with rBCG expands the central memory compartment of antigen (Ag)–specific CD4⁺ T cells. *A–C*, Data from pooled lymphoid organs from individual mice at day 14 after receipt of BCG or rBCG. *A*, Representative flow cytometry results showing memory markers gated on CD3⁺CD4⁺Ag85B:I-Ab⁺ T cells enriched from vaccinated or naive control mice. *B*, Surface CCR7 or nuclear Bcl-6 expression on representative naive CD3⁺CD4⁺Ag85B:I-Ab⁺ populations or CCR7⁻CXCR5⁻PD1⁻ (T_{EM}), CCR7⁺CXCR5⁺PD1⁻ (T_{CM}), and CCR7⁺CXCR5^hiPD1^hi (T_{FH}) populations from rBCG recipients. *C*, Intracellular expression of transcription factors by CD3⁺CD4⁺Ag85B:I-Ab⁺ in naive mice, BCG recipients, or rBCG recipients. *D*, Mean total numbers (± standard error of the mean) of CD3⁺CD4⁺Ag85B:I-Ab⁺ T_{EM}, T_{CM}, and T_{FH} gated as in panel *B* and enriched from pooled lymphoid organs from individual animals following vaccination. *E*, Mean frequency of effector populations among Ag85B:I-Ab⁺ CD4⁺ T cells gated as in panel *B*, 90 days after vaccination. Data are representative values from 3 independent experiments (*A–C*) or pooled values from 2–3 experiments (*D* and *E*; n = 6–10). *$P < .05$, **$P < .01$, and ***$P < .001$, by a 2-tailed Student *t* test.

T_{CM} (Figure 4*C* and 4*D*). The T_{FH} population was also increased following rBCG but not BCG receipt but gradually contracted to preimmunization levels by day 90 and was thus unlikely to play a role in recall responses in this model (Figure 4*C* and 4*D*). The expanded Ag-specific T_{CM} population after rBCG vaccination was thus a potential correlate of protection against pulmonary tuberculosis.

rBCG Induces Enhanced Ab Production to Mycobacterial Ag

The T_{FH} population stimulates germinal center B-cell responses [25], but the role of B cells and Ab in tuberculosis remains incompletely understood [26, 27]. We therefore verified the functionality of the increased Ag-specific T_{FH} population following rBCG receipt by examining sera obtained from vaccinated mice

for Ab, using an *M. tuberculosis* protein lysate ELISA. We observed significantly higher serum reactivity in rBCG recipients, compared with BCG recipients, by 1 month after vaccination, which persisted as long as 3 months later (Figure 5*A*). This response was dominated by class switch to the immunoglobulin (Ig) G2c and IgG2b isotypes, although the IgG1 level was also increased to some extent (Figure 5*A* and Supplementary Figure 2). In contrast, Ig M levels were similar in all groups, and specific Ig A was not detected (Supplementary Figure 2 and data not shown). Therefore, rBCG induced Ab with high efficacy. Intriguingly, preexisting specific Ab induced by rBCG persisted after aerosol challenge with *M. tuberculosis* 3 months after vaccination, and levels remained markedly higher 28 days following infection, compared with levels in both untreated mice
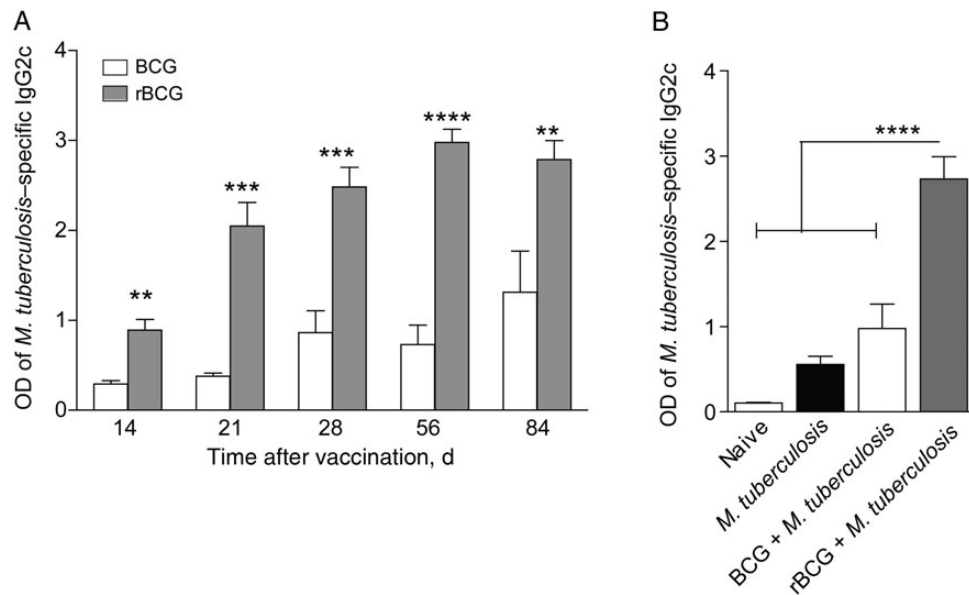
Figure 5. Vaccination with rBCG induces increased production of *Mycobacterium tuberculosis*–reactive antibody, compared with BCG. Mice were vaccinated with BCG or rBCG and were challenged 3 months later with a low dose of *M. tuberculosis*, alongside naive controls. The OD of *M. tuberculosis*–reactive immunoglobulin G2c (IgG2c) in sera, measured by enzyme-linked immunosorbent assay, in BCG and rBCG recipients (*A*) or in naive mice, *M. tuberculosis* recipients, BCG plus *M. tuberculosis* recipients, and rBCG plus *M. tuberculosis* recipients. Data show mean pooled values (± standard error of the mean) from 2 experiments (n = 10). **P < .01***P < .001, and ****P < .0001, by 1-tailed analysis of variance, followed by the Bonferroni posttest.

and BCG recipients (Figure 5*B*). To determine whether increased mycobacteria-specific Ab was protective, we passively transferred serum from BCG recipients and rBCG recipients into naive animals but did not detect impact on tuberculosis (Supplementary Figure 2).

rBCG Provides Improved Protection Against Pulmonary Tuberculosis

We interrogated whether the enhanced T_{CM} persistence after rBCG receipt correlated with improved T-cell recruitment to the lung after challenge with *M. tuberculosis*. To this end, we challenged vaccinated mice with a low dose of aerosolized *M. tuberculosis* 3 months after vaccination. As shown previously for BALB/c mice, rBCG-recipient C57BL/6 mice showed superior protection in the lung over BCG recipients, particularly late in infection (Figure 6*A*) [15, 28], but dissemination of *M. tuberculosis* to the spleen and liver was similar (Supplementary Figure 3). T_M are thought to rapidly expand in the LNs and subsequently migrate to the lung before their naive counterparts when reexposed to Ag. To determine whether T_M recall responses to Ag85B were increased in the lung, cell isolation was performed on day 14, the earliest time point at which T cells are recruited to the periphery in murine tuberculosis, where they provide a brake on bacterial growth and lung pathology [29]. We did not detect significantly increased Ag85B-specific CD4$^+$ T-cell recruitment to the spleen or lung

at day 14 in vaccinated or unvaccinated mice (Figure 6*B*). We also quantified the primary CD4$^+$ T-cell response to *M. tuberculosis* early secreted Ag-6 (ESAT-6; Rv3875), which is not expressed by BCG, as well as total CD4$^+$ T-cell numbers in the lung. Again, the number of primary CD4$^+$ T cells specific to ESAT-6 were similar between all groups at day 14 following *M. tuberculosis* infection (Figure 6*B*). Thus, quantitative differences in Ag-specific T-cell responses did not underlie the superior protection against tuberculosis induced by rBCG, compared with BCG.

Adoptive Transfer of T_{CM} Rather Than T_{EM} Protects Against Tuberculosis

To compare differential protection by endogenous Ag-specific T_M subsets, we designed an adoptive T-cell transfer system that removed confounding effects by Ab, memory and plasma B cells, CD8$^+$ T cells, or other innate and adaptive components of memory that may arise after vaccination (Figure 7*A*) [29, 30]. Congenic mice expressing the discriminatory CD90.1 marker received rBCG, and the polyclonal Ag85B:I-Ab$^+$ T-cell population was purified into either T_{EM} (8000 per recipient) or T_{CM}/T_{FH} (2000 per recipient) by FACS before intravenous transfer to naive C57BL/6 recipients (Figure 7*B*). Assuming a so-called park rate of approximately 10% of transferred cells, this approach was predicted to result in establishment of approximately 200 T_{CM} or 1000 T_{EM} in the lymphatics of recipient mice, equivalent to the number of endogenous Ag85B-specific cells we had observed 90 days after rBCG receipt (Figure 4). After resting for 2–3 days
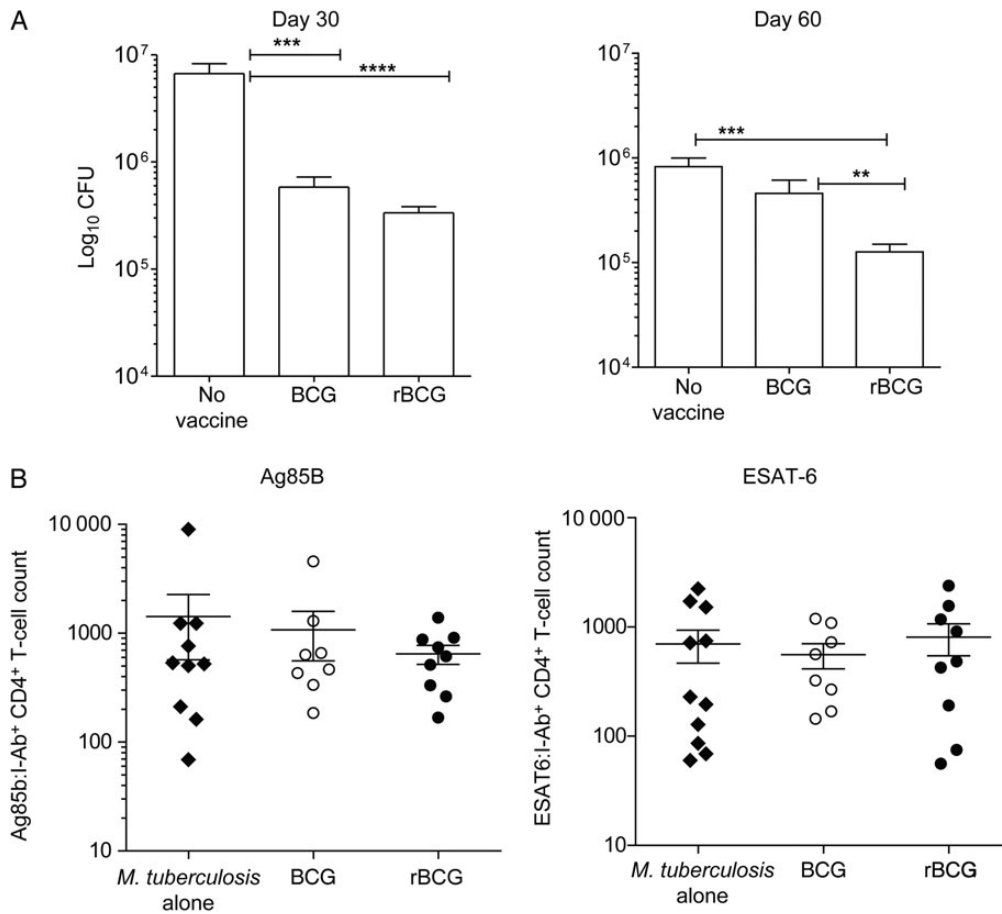
Figure 6. Vaccination with rBCG induces superior protection over BCG in the lung despite similar CD4$^+$ T-cell recruitment at early time points after *Mycobacterium tuberculosis* infection. Mice were vaccinated and challenged with *M. tuberculosis* as described in Figure 5. *A*, *M. tuberculosis* colony-forming units (CFU) in lungs 30 and 60 days following *M. tuberculosis* challenge. *B* and *C*, Total numbers of memory Ag85B:I-Ab$^+$ (*B*) and primary (*C*) ESAT6:I-Ab$^+$ CD4$^+$ T cells in lungs, quantified by flow cytometry, 14 days after *M. tuberculosis* infection. All graphs show mean ± standard error of the mean of pooled values from 2 experiments (n = 10). **$P < .01$, ***$P < .001$, and ****$P < .0001$, by the Mann–Whitney *U* test.

without Ag to favor a memory phenotype, recipient mice were challenged with aerosolized *M. tuberculosis*. Bacterial load was determined 21 days later. The donor memory T_{EM} and T_{CM}/T_{FH} compartments were enumerated by flow cytometry in spleen and lung by means of CD90.1. Both populations survived and proliferated to a similar extent following *M. tuberculosis* challenge (Figure 7*C*). Transferred T_{CM}/T_{FH} significantly decreased the *M. tuberculosis* burden, with the strongest effect in the lung and a trend toward reduced dissemination to other organs (Figure 7*D*). To determine whether protection was mediated by T_{CM} or T_{FH}, we established an alternative double adoptive transfer system capable of inducing larger numbers of responding T cells than could be practically isolated from the polyclonal endogenous repertoire. We first transferred naive CD4$^+$ T cells from T-cell receptor–transgenic P25 donor mice recognizing the same Ag85B epitope as the endogenous tetramer$^+$ population. Naive recipients were then primed with rBCG to allow FACS separation of rare Ag-specific T_{EM}, T_{CM}, and T_{FH} for transfer into

C57BL/6 mice prior to *M. tuberculosis* infection (Figure 7*E*). Intriguingly, transfer of purified P25 transgenic T_{CM} markedly protected against tuberculosis, in contrast to naive, T_{EM}, or T_{FH} counterparts (Figure 7*F*). Thus, protection by rBCG primarily resided in the T_{CM} population in this adoptive transfer system.

DISCUSSION

Recent interest has focused on T_{CM} as mediators of protection following vaccination with protein–adjuvant formulations as heterologous boosters. For example, LN-resident cells that were CD62L$^+$CCR7$^+$ and secreted interleukin 2 (IL-2) controlled *M. tuberculosis* upon transfer into immunodeficient mice [9]. Multifunctional T_{CM}-like IL-2/TNF-α/IFN-γ$^+$ cells have also been associated with protection following vaccination [31–34]. In humans, increasing evidence points to an association between *M. tuberculosis*–specific T_{CM} in peripheral blood
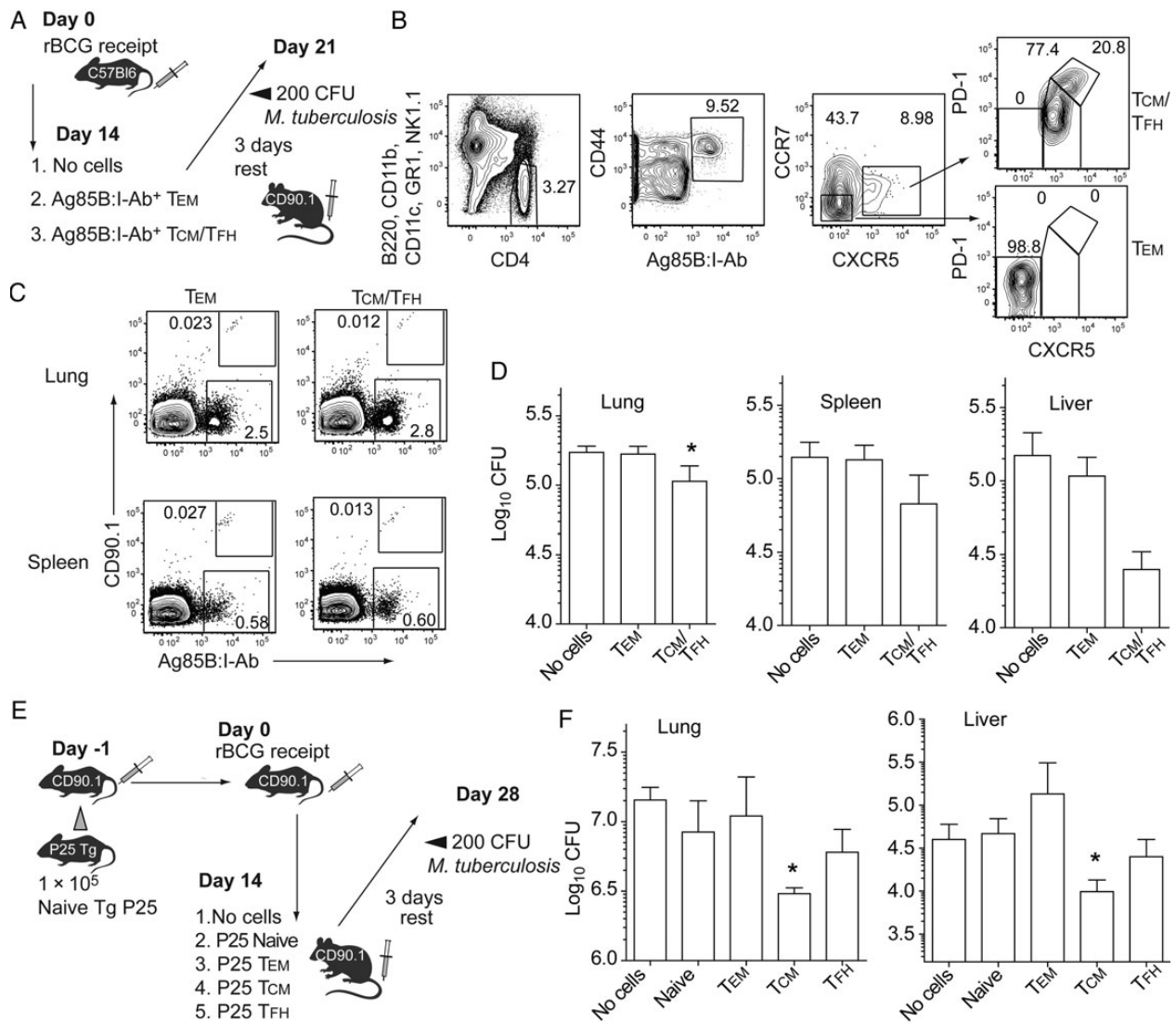
Figure 7. Adoptively transferred Ag85B-specific central memory CD4$^+$ T cells (T$_{CM}$) induced by rBCG protect against tuberculosis. *A*, Adoptive transfer strategy. Endogenous Ag85B-specific effector memory CD4$^+$ T cells (T$_{EM}$; CCR7$^-$CXCR5$^-$PD-1$^-$; 8000 per recipient) and T$_{CM}$/T follicular helper T cells (T$_{FH}$; CCR7$^+$CXCR5$^+$PD-1$^+$; 3000 per recipient) were FACS purified from rBCG vaccinated, congenic CD90.1$^+$ mice and then transferred into naive C57BL/6 recipients. After 3 days of rest, recipients and controls were infected with low-dose aerosolized *Mycobacterium tuberculosis* and analyzed 21 days after infection. *B*, Cell-sorting strategy to separate CD4$^+$Ag85B:I-Ab$^+$ cells into T$_{EM}$ and T$_{CM}$/T$_{FH}$ subsets as in panel *A*, and postsort expression of T$_{FH}$ markers prior to transfer (right). *C*, Representative flow cytometry of CD90.1$^+$ donor T$_{EM}$ or T$_{CM}$/T$_{FH}$ after *M. tuberculosis* infection as in panel *A*, gated on total CD3$^+$CD4$^+$ cells in recipients of adoptive cell transfer. *D*, *M. tuberculosis* colony-forming units (CFU) after infection as in panel *A*. *E*, Second adoptive transfer strategy. A total of 1×10^5 naive P25 Tg T cells were transferred into naive mice, which were then vaccinated with rBCG. Fourteen days later, donor cells were isolated by FACS and separated into T$_{EM}$ (CCR7$^-$CXCR5$^-$PD-1$^-$; 8000 per recipient), T$_{CM}$ (CCR7$^+$CXCR5$^+$PD-1$^-$; 3000 per recipient), and T$_{FH}$ (CCR7$^+$CXCR5$^+$PD-1$^+$; 2000 per recipient) for transfer into naive mice. After 3 days of rest, recipients of adoptive cell transfer and controls were infected with low-dose aerosolized *M. tuberculosis* and analyzed 28 days after infection. *F*, CFU after *M. tuberculosis* infection as in panel *E*. Data show mean values (± standard error of the mean) representative of 2 experiments (n = 3–6). *$P < .05$, by the Mann–Whitney *U* test.

and latent *M. tuberculosis* infection, rather than progression to active tuberculosis [35, 36]. Whether the ability to produce this polyfunctional cytokine profile upon restimulation is inherently protective in the lung or merely allows identification of T$_{CM}$ with the capacity to generate a variety of different progeny during recall is the focus of ongoing studies. Our results

demonstrate that rBCG induced higher absolute numbers and proportions of Ag-specific T$_{CM}$ than BCG, with characteristic CXCR5$^+$CCR7$^+$ expression and an absence of effector transcription factors. Elevated T$_{CM}$ numbers and proportions were evident at the peak of the response and were maintained after clearance of rBCG, suggesting that these cells arise during

the T_H expansion but, unlike T_{FH}, persist throughout the contraction phase to become T_{CM}. Adoptive transfer of T_{CM} or cotransfer of T_{CM} and T_{FH} specific for a single mycobacterial Ag shared between rBCG and *M. tuberculosis*, Ag85B, sufficed for profound protection against pulmonary tuberculosis. T_{FH} alone were unable to significantly reproduce this effect, yet it is possible that these cells could inhibit *M. tuberculosis* if higher numbers were transferred. T_{CM} have been shown to generate a second wave of Ag-specific T_{FH} following reexposure to Ag, and this may also occur when BCG vaccination is followed by infection with *M. tuberculosis* [35]. Further transcriptome analysis of Ag-specific T_M may reveal further qualitative differences between memory subsets that were not observed in this study.

In mice and humans, circulating T_{CM} and T_{FH} both express CXCR5 and are frequently associated with enhanced Ab responses to infection [18, 37, 38]. Recent studies emphasized the importance of CXCR5 expression on mycobacteria-specific T cells for migration to organized lymphoid structures in the lung containing B cells in mouse, human, and nonhuman primate tuberculosis [39–41]. These structures and prevalent CXCR5-expressing T cells have been correlated with decreased lung pathology following vaccination and challenge with *M. tuberculosis*, rather than canonical Th1 or T_{EM} responses [42, 43]. It remains to be determined whether rBCG is associated with the development of ectopic lymphoid structures comprising T cells, B cells, and macrophages in the lung.

Intriguingly, enhanced production of mycobacterial Ag-specific Ab was a strong differentiating factor of the immune response to rBCG, compared with the response to BCG, in a phase 1 clinical trial [16]. We identified a profound increase in T_{FH} and associated Ab production following rBCG receipt, compared with BCG receipt, as well as formation of germinal centers in draining LNs (data not shown). Secreted protein Ag are preferred targets of both B and T cells in tuberculosis [35]. Therefore, increased B-cell activation following rBCG receipt may facilitate collaboration for cognate Ag presentation. Indeed, polyfunctional T_{CM} and T_{FH} both uniquely depend on strong T-cell receptor signals for their development [44–46]. Alternatively, complexes derived from Ab and mycobacterial Ag captured by follicular dendritic cells in long-lasting germinal centers could favor differentiation of protective T_{CM} and T_{FH}. In murine *Listeria monocytogenes* and lymphocytic choriomeningitis virus infection, Ag presentation by B cells is directly correlated with increased differentiation of monoclonal transgenic T cells into T_{CM} and T_{FH} phenotypes [18, 47]. More recently, marked T_{FH} responses were found to correlate with development of broadly neutralizing Ab to HIV or autoantibodies in humans [37, 48].

In conclusion, our findings reveal that receipt of rBCG induces a superior Ag-specific T_{CM} response over BCG, which contributes to protection against tuberculosis. Novel tuberculosis prime or boost strategies should target the expansion of this

T_{CM} subset, with the aim of improving long-lasting protection. Moreover, our results emphasize the potential usefulness of the rBCG expressing heterologous Ag from pathogens that are more susceptible to neutralizing Ab, owing to its safety and targeted activation of sustained T_{FH} and B-cell immunity.

Notes

References

1. Calmette A, Plotz H. Protective inoculation against tuberculosis with BCG. Am Rev Tuberc **1929**; 19:567–72.
2. Andersen P, Doherty TM. The success and failure of BCG - implications for a novel tuberculosis vaccine. Nat Rev Microbiol **2005**; 3:656–62.
3. Kaufmann SH. Tuberculosis vaccines: time to think about the next generation. Semin Immunol **2013**; 25:172–81.
4. Kaufmann SH. Fact and fiction in tuberculosis vaccine research: 10 years later. Lancet Infect Dis **2011**; 11:633–40.
5. Orme IM. Characteristics and specificity of acquired immunologic memory to *Mycobacterium tuberculosis* infection. J Immunol **1988**; 140:3589–93.
6. Orme IM, Collins FM. Adoptive protection of the *Mycobacterium tuberculosis*-infected lung. Dissociation between cells that passively transfer protective immunity and those that transfer delayed-type hypersensitivity to tuberculin. Cell Immunol **1984**; 84:113–20.
7. Bold TD, Banaei N, Wolf AJ, Ernst JD. Suboptimal activation of antigen-specific CD4+ effector cells enables persistence of *M. tuberculosis* in vivo. PLoS Pathog **2011**; 7:e1002063.
8. Tamura T, Ariga H, Kinashi T, et al. The role of antigenic peptide in CD4+ T helper phenotype development in a T cell receptor transgenic model. Int Immunol **2004**; 16:1691–9.
9. Andersen P, Smedegaard B. CD4(+) T-cell subsets that mediate immunological memory to *Mycobacterium tuberculosis* infection in mice. Infect Immun **2000**; 68:621–9.
10. Seder RA, Darrah PA, Roederer M. T-cell quality in memory and protection: implications for vaccine design. Nat Rev Immunol **2008**; 8:247–58.
11. Torrado E, Cooper AM. What do we really know about how CD4 T cells control *Mycobacterium tuberculosis*?. PLoS Pathog **2011**; 7:e1002196.
12. Abebe F. Is interferon-gamma the right marker for bacille Calmette-Guerin-induced immune protection? The missing link in our understanding of tuberculosis immunology. Clin Exp Immunol **2012**; 169:213–9.

13. Pollock KM, Whitworth HS, Montamat-Sicotte DJ, et al. T-cell immunophenotyping distinguishes active from latent tuberculosis. J Infect Dis **2013**; 208:952–68.

14. Ottenhoff TH, Spierings E, Nibbering PH, de JR. Modulation of protective and pathological immunity in mycobacterial infections. Int Arch Allergy Immunol **1997**; 113:400–8.

15. Grode L, Seiler P, Baumann S, et al. Increased vaccine efficacy against tuberculosis of recombinant *Mycobacterium bovis* bacille Calmette-Guerin mutants that secrete listeriolysin. J Clin Invest **2005**; 115:2472–9.

16. Grode L, Ganoza CA, Brohm C, Weiner J III, Eisele B, Kaufmann SH. Safety and immunogenicity of the recombinant BCG vaccine VPM1002 in a phase 1 open-label randomized clinical trial. Vaccine **2013**; 31:1340–8.

17. Rao M, Vogelzang A, Kaiser P, Schuerer S, Kaufmann SH, Gengenbacher M. The tuberculosis vaccine candidate Bacillus Calmette-Guerin deltaureC::hly coexpressing human interleukin-7 or -18 enhances antigen-specific T cell responses in mice. PLoS One **2013**; 8:e78966.

18. Pepper M, Pagan AJ, Igyarto BZ, Taylor JJ, Jenkins MK. Opposing signals from the Bcl6 transcription factor and the interleukin-2 receptor generate T helper 1 central and effector memory cells. Immunity **2011**; 35:583–95.

19. Cooper AM, Khader SA. The role of cytokines in the initiation, expansion, and control of cellular immunity to tuberculosis. Immunol Rev **2008**; 226:191–204.

20. Kirchhoff D, Frentsch M, Leclerk P, et al. Identification and isolation of murine antigen-reactive T cells according to CD154 expression. Eur J Immunol **2007**; 37:2370–7.

21. Linterman MA, Liston A, Vinuesa CG. T-follicular helper cell differentiation and the co-option of this pathway by non-helper cells. Immunol Rev **2012**; 247:143–59.

22. Zhang WX, Yang SY. Cloning and characterization of a new member of the T-box gene family. Genomics **2000**; 70:41–8.

23. Egen JG, Rothfuchs AG, Feng CG, Horwitz MA, Sher A, Germain RN. Intravital imaging reveals limited antigen presentation and T cell effector function in mycobacterial granulomas. Immunity **2011**; 34:807–19.

24. Zhu J, Yamane H, Paul WE. Differentiation of effector CD4+ T cell populations (*). Annu Rev Immunol **2010**; 28:445–89.

25. Liu SM, King C. IL-21-producing Th cells in immunity and autoimmunity. J Immunol **2013**; 191:3501–6.

26. Greif F, Sharon E, Shechtman I, Morgenstern S, Gutman H. Carcinoma within solitary ductal papilloma of the breast. Eur J Surg Oncol **2010**; 36:384–6.

27. Kozakiewicz L, Phuah J, Flynn J, Chan J. The role of B cells and humoral immunity in *Mycobacterium tuberculosis* infection. Adv Exp Med Biol **2013**; 783:225–50.

28. Desel C, Dorhoi A, Bandermann S, Grode L, Eisele B, Kaufmann SH. Recombinant BCG DeltaureC hly+ induces superior protection over parental BCG by stimulating a balanced combination of type 1 and type 17 cytokine responses. J Infect Dis **2011**; 204:1573–84.

29. Cooper AM. Cell-mediated immune responses in tuberculosis. Annu Rev Immunol **2009**; 27:393–422.

30. Sebina I, Cliff JM, Smith SG, et al. Long-lived memory B-cell responses following BCG vaccination. PLoS One **2012**; 7:e51381.

31. Derrick SC, Yabe IM, Yang A, Morris SL. Vaccine-induced anti-tuberculosis protective immunity in mice correlates with the magnitude and quality of multifunctional CD4+ T cells. Vaccine **2011**; 29:2902–9.

32. Lindenstrom T, Knudsen NP, Agger EM, Andersen P. Control of chronic *Mycobacterium tuberculosis* infection by CD4 KLRG1- IL-2-secreting central memory cells. J Immunol **2013**; 190:6311–9.

33. Forbes EK, Sander C, Ronan EO, et al. Multifunctional, high-level cytokine-producing Th1 cells in the lung, but not spleen, correlate with protection against *Mycobacterium tuberculosis* aerosol challenge in mice. J Immunol **2008**; 181:4955–64.

34. Lindenstrom T, Agger EM, Korsholm KS, et al. Tuberculosis subunit vaccination provides long-term protective immunity characterized by multifunctional CD4 memory T cells. J Immunol **2009**; 182:8047–55.

35. Lindestam Arleharn CS, Gerasimova A, Mele F, et al. Memory T cells in latent *Mycobacterium tuberculosis* infection are directed against three antigenic islands and largely contained in a CXCR3+CCR6+ Th1 subset. PLoS Pathog **2013**; 9:e1003130.

36. Biselli R, Mariotti S, Sargentini V, et al. Detection of interleukin-2 in addition to interferon-gamma discriminates active tuberculosis patients, latently infected individuals, and controls. Clin Microbiol Infect **2010**; 16:1282–4.

37. He J, Tsai LM, Leong YA, et al. Circulating precursor CCR7(lo)PD-1(hi) CXCR5(+) CD4(+) T cells indicate Tfh cell activity and promote antibody responses upon antigen reexposure. Immunity **2013**; 39:770–81.

38. Chevalier N, Jarrossay D, Ho E, et al. CXCR5 expressing human central memory CD4+ T cells and their relevance for humoral immune responses. J Immunol **2011**; 186:5556–68.

39. Kahnert A, Hopken UE, Stein M, Bandermann S, Lipp M, Kaufmann SH. *Mycobacterium tuberculosis* triggers formation of lymphoid structure in murine lungs. J Infect Dis **2007**; 195:46–54.

40. Ulrichs T, Kosmiadi GA, Trusov V, et al. Human tuberculous granulomas induce peripheral lymphoid follicle-like structures to orchestrate local host defence in the lung. J Pathol **2004**; 204:217–28.

41. Phuah JY, Mattila JT, Lin PL, Flynn JL. Activated B cells in the granulomas of nonhuman primates infected with *Mycobacterium tuberculosis*. Am J Pathol **2012**; 181:508–14.

42. Gopal R, Rangel-Moreno J, Slight S, et al. Interleukin-17-dependent CXCL13 mediates mucosal vaccine-induced immunity against tuberculosis. Mucosal Immunol **2013**; 6:972–84.

43. Slight SR, Rangel-Moreno J, Gopal R, et al. CXCR5(+) T helper cells mediate protective immunity against tuberculosis. J Clin Invest **2013**; 123:712–26.

44. Fazilleau N, McHeyzer-Williams LJ, Rosen H, McHeyzer-Williams MG. The function of follicular helper T cells is regulated by the strength of T cell antigen receptor binding. Nat Immunol **2009**; 10:375–84.

45. Ma CS, Suryani S, Avery DT, et al. Early commitment of naive human CD4(+) T cells to the T follicular helper (T(FH)) cell lineage is induced by IL-12. Immunol Cell Biol **2009**; 87:590–600.

46. Tubo NJ, Pagan AJ, Taylor JJ, et al. Single naive CD4+ T cells from a diverse repertoire produce different effector cell types during infection. Cell **2013**; 153:785–96.

47. Whitmire JK, Asano MS, Kaech SM, et al. Requirement of B cells for generating CD4+ T cell memory. J Immunol **2009**; 182:1868–76.

48. Locci M, Havenar-Daughton C, Landais E, et al. Human circulating PD-(+)1CXCR3(-)CXCR5(+) memory Tfh cells are highly functional and correlate with broadly neutralizing HIV antibody responses. Immunity **2013**; 39:758–69.